

## UV RADIATION IN THE SOUTHERN SEAS IN SUMMER 2000

Gerd Wendler and Brian Hartmann

Geophysical Institute, University of Alaska, Fairbanks, Alaska 99775

### Abstract

During a cruise on the *USCGC POLAR SEA* from Hobart, Tasmania to McMurdo, Antarctica, continuous radiation measurements were carried out; the global, UV-A and UV-B are being discussed in this paper. As we were performing the measurements on a moving platform, spot measurements can be incorrect, however, for hourly means the validity was confirmed. It was found that the radiation levels decreased at noon when going South, however, the mean daily flux increased on average, as the reduced radiation at noon was overcompensated by longer day length. For the day-to-day variations, the amount of cloudiness was of greatest importance. The mean value of the clearness index  $K_t$  (total transmissivity) was found to be 0.51, a somewhat low value, which was caused by the high mean amount of cloudiness, mostly consisting of stratus. The mean clearness index was 0.74 for clear skies and 0.38 for overcast conditions, while individual values varied even more.

The UV radiation can be related to the global radiation. However, correlation coefficients improved substantially when the analyses were done for different cloudiness classes. Clouds produced the largest reduction for the global radiation, followed by UV-A and the UV-B. With other

words, the relative intensity of UVB was influenced the least by clouds. No good correlations between total ozone and UVB could be established, as the Antarctic ozone hole, which was well developed in spring, had been filled and values above 300 DU (Dobson Units) were observed during the whole passage.

### 1. Introduction

Ultraviolet radiation contributes relatively little energy to the solar spectrum; however, it is of high importance as it is biologically very active (e.g. Buckley and Trodahl 1990). On 14 December 2000, the *USCGC POLAR SEA* left Hobart, Tasmania, for a trip to McMurdo, Antarctica. Its primary mission was the opening of McMurdo Sound to tanker and ship traffic. The route of the ship, as well as the sea ice edge as of 22 December 2000 is shown in Figure 1. On 17 December 2000 we observed the first sea ice from the ship. The following day, helicopter operations were conducted to Dumont d'Urville, the primary French Antarctic station, to bring supply parts for automatic weather stations (AWS), which report via satellite year-round. During the next 3 days, we serviced AWS's along the Adélie and King George Coasts (Stearns and Wendler, 1988), and thereafter continued our voyage arriving at McMurdo on 1 January 2001. During this trip we carried out continuous meteorological and radiative measurements from the ship, supported by visual hourly observations of cloudiness and sea ice concentration.

---

*Corresponding author.* Gerd Wendler,  
Geophysical Institute, University of Alaska,  
Fairbanks, Alaska, 99775 email:  
gwendler@gi.alaska.edu

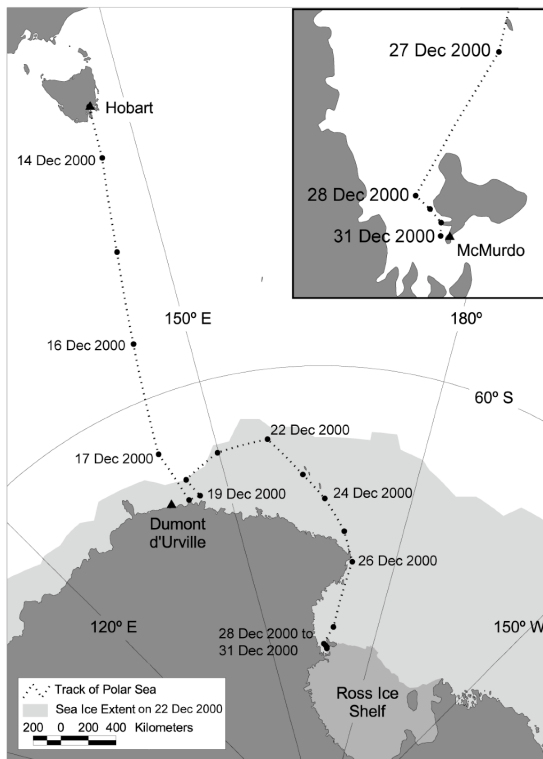


**Figure 1.** The trip of the USCGC POLAR SEA from Hobart, Tasmania, to McMurdo, Antarctica, during the 2000/2001 voyage. The position of the ship is given daily at noon, as well as the ice edge surrounding Antarctica as of 22 December 2000.

## 2. Measurements and meteorological conditions

In a previous investigation (Wendler et al., 2004), we reported on the effect of multiple reflection on the net radiation. Here we present the UV radiative measurements as a function of the solar elevation and cloudiness. We installed on the fly-bridge, about 32 m above the ocean surface, the UV and total global radiation sensors (Figure 2). The UV-A radiation was measured with an Eppley instrument (sensitivity 290-385 nm), the UV-B radiation with a Yankee Environmental System instrument

(sensitivity 285-330nm), and the global radiation with an Eppley PSP (sensitivity 385-780nm).



**Figure 2.** Radiation equipment installed on the fly-bridge of the USCGC POLAR SE. Right to left: UV-B Yankee Environmental System, Eppley PIR (infrared), Eppley UV-A, Eppley PSP (visible). The sea ice concentration is 8/10.

A notebook computer allowed access to the data in real or near-real time so that the data quality could be checked at any time and instrumentation breakdown could be detected and addressed without large time delays. It should be pointed out that such a voyage is tough on instrumentation, as we are crossing one of the roughest seas (the Roaring Forties) with an abundance of spray in the air. After drying, sea salt accumulates requiring that the domes of the radiation instrumentation be cleaned frequently. This was carried out systematically twice

daily, and more often when conditions demanded this. No correction was carried out for it. When within the ice pack, the swell declines. However, the mechanical action of ice breaking can be severe, and the shocks are transmitted to the instrumentation.

All instruments were sampled in 20-second intervals and averaged into 5-minute resolution data, and recorded on a Campbell Scientific 21X data logger. The only exception in recording were pitch and roll, for which we measured the standard deviation for each 5 minute interval, as the mean would have given values close to zero. We tested the radiation data against increasing standard deviation in pitch and roll, using four pitch and six roll classes. While there was a substantial scatter within each class, no systematic increase with increasing ship movement could be detected for hourly values. We deduced that the movement of the ship did not affect hourly radiative measurements. This might be in part due to the fact that increasing wave actions normally occur during stormy periods, during which high amounts of cloudiness is observed. During overcast condition only diffuse radiation is observed which is less affected by deviation from the horizontal surface than direct radiation.

In addition to these measurements hourly data of all standard meteorological conditions, including cloud amount and type and sea ice conditions, was carried out by the Marine Science Technicians on board the *POLAR SEA*. This was a continuous effort during the whole trip. Further, an online digital camera was installed at the crow's nest looking forward, taking imagery every two

minutes. This imagery was stored and films were later on produced, which allowed the observations of sudden changes in ice concentration and type, and to a lesser extend of cloud conditions on a finer time scale than the hourly observations.

When leaving Hobart, Tasmania, on 14 December, the air temperature was around 15°C, and during the next 3 days the temperature decreased steadily. On 17 December the first ice became visible and the temperature hovered near the melting point of sea ice (about -1.8°C) until we reached McMurdo Sound on 28 December. Here, due to the absence of the moderating effect of open water, the diurnal temperature variation increased and night temperatures dropped to -8°C. The humidity was high during the whole trip with values of about 80% relative humidity, typical for a marine environment. Overcast conditions were dominant during the whole trip, mostly consisting of polar stratus clouds. The lowest atmospheric pressure was observed on 24 December (982 hPa) and the following day wind speeds in excess of 25 ms<sup>-1</sup> were observed. For the first 4 days, no sea ice was observed, thereafter the ice concentration varied widely, until we reached the solidly frozen McMurdo Sound.

### 3. Results

While the radiative intensity at noon decreased when going to higher latitudes due to the decreasing solar elevation, the mean daily flux increased as the length of daylight overcompensated this loss. In Figure 3 the global radiation, UV-A and UV-B are plotted against solar elevation. Naturally, the absolute magnitude of the

radiative fluxes is very different for the 3 wavelength classes. In all cases, a large amount of scatter is being observed, a result to be expected, as we did not stratify the data by cloud amount and cloud type. Maybe the most striking difference is the less pronounced dependency of UV-B radiation on the solar elevation when compared with the global and UV-A radiation.

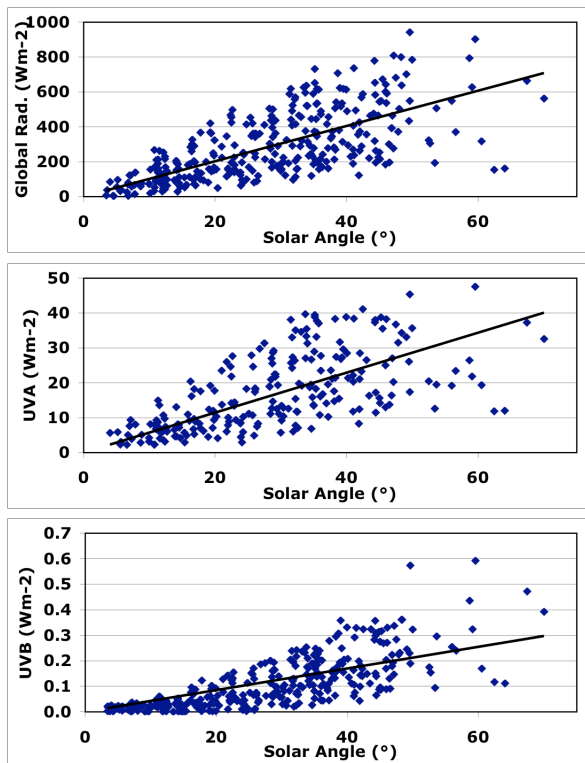


**Figure 3.** Global, UV-A and UV-B radiation fluxes as function of solar elevation

In Figure 4 we present the total transmissivity ( $K_T$ ) of the atmosphere as function of cloudiness. It represents the ratio of the amount of radiation at the surface to the amount received on the top of the atmosphere and is also sometimes called clearness index. There is a large amount of variation, as it depends on the

cloud type (e.g. Vowinkel and Orvig 1962).

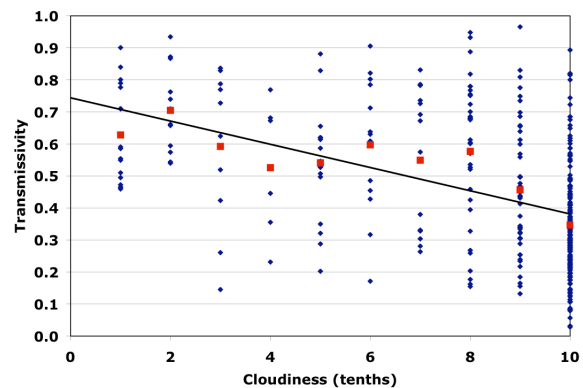


**Figure 4.** The total transmissivity ( $K_T$ ) of the atmosphere is plotted against cloud amount. Note the decrease of  $K_T$  with increasing cloudiness.

Further, for partial cloud cover, the fact that a cloud is in the path of the solar rays is of greatest importance. In general we can see an increase of total transmissivity with increasing cloud amount. For total overcast, 38%, and for clear sky conditions 74% from the energy received on top of the atmosphere reach the surface. The mean value of all observations was just above half (51%).

In Figure 5, the global, UV-A and UV-B radiation is presented as function of cloud amount. For all cases an increase in the radiative fluxes with decreasing cloudiness can be observed, even though there is a large amount of scatter. Hourly data presented here are for an air mass of  $< 2$ , hence the path length through the atmosphere does not vary very widely. However, we did not distinguish between cloud types, and even for one specific cloud type, there can be a large variation in thickness, droplet or ice crystal numbers and size distribution.

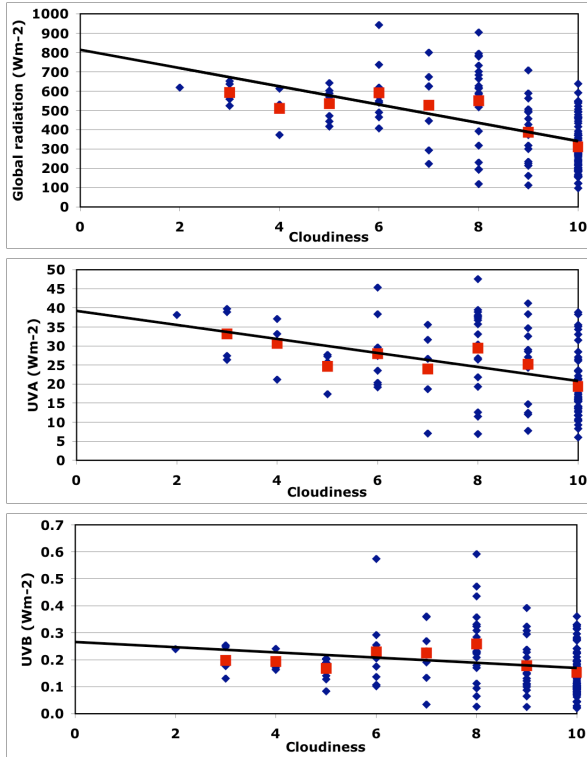


**Figure 5.** Global, UV-A and UV-B radiation as function of cloud amount.

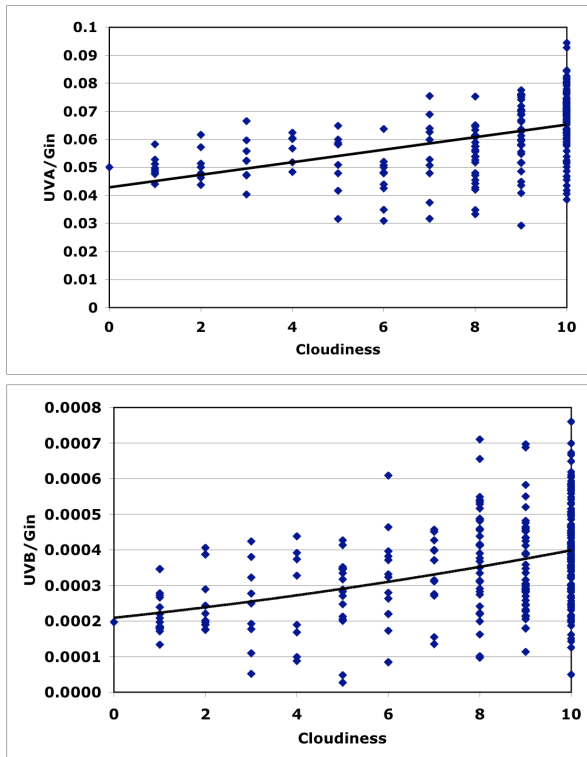


**Figure 6.** The relative abundance of UV-A and UV-B radiation when compared to the total global radiation.

In general it can be seen, that the decrease of the radiative flux with increasing cloudiness is strongest in the visible region, followed by UV-A and UV-B. With other words, the visible region of the solar spectrum is to a greater extent reflected back to space or absorbed by the clouds when compared with the UV radiation. This fact can be better judged from Figure 6, in which the relative abundance of UV-A and UV-B radiation of the total incoming radiation is presented. It can be seen that for clear sky conditions, the UV-A part represents 4.3%, while for total overcast this value increased to 6.4%. Such a relative increase is even more pronounced in the UV-B region of the spectrum, where the value nearly doubles, from 0.022% to 0.040%.

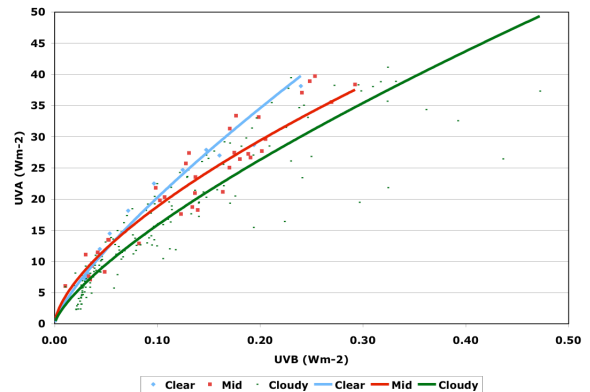


**Figure 7.** UV-A vs. UV-B as a function of cloud amount

We plotted the intensities of UV-A and UV-B radiation against each other. Lots of scatter was observed. Hence, we stratified the data set into 3 classes, namely clear (<3/10), partly cloudy (3-8/10) and overcast (>8/10). The results are presented in Figure 7, from which can be seen that for the same intensity in the UV-A, the UV-B increases with increasing cloudiness.

Finally, we looked at the Total Ozone Mapping Spectrometer (TOMS) data, which represent the total ozone amount of the atmosphere as measured by satellite. One would expect that the visible and UV-A are hardly affected by it, however the UV-B should show a strong dependence from the ozone amount, as has been previously shown (Farman et al.1985). However, no good correlations between total ozone and UV-B could be established, as the Antarctic ozone hole, which is normally well developed in spring (e.g. Wendler and Quackenbush 1996), had been filled and values above 300 DU (Dobson Units) were observed during the whole passage.

### **Acknowledgement**

The research was supported by NSF grant OPP 97-25843 and the Alaska Climate Research Center. Captain Keith Johnson, XO Steve Wheeler and the whole crew of the *POLAR SEA* supported us wonderfully. Special thanks go also to the marine science technicians and the helicopter detachment. R. Flint and B. Moore who took part in the cruise, kept all the instrumentation running.

### **References**

- Ambach, W., M. Blumthaler and G. Wendler 1991: A comparison of ultraviolet radiation measured at an arctic and an alpine site. *Solar Energy*, **47**, No 2, 121-126
- Buckley, R. and H. Trodahl 1990: Radiation risk. *Nature*, **346**, 6279
- Farman, J., B. Gardiner and J. Shanklin 1985: Large losses of total ozone in Antarctica reveals seasonal ClOx/NOx interactions. *Nature* **315**. 207-210
- Stearns, C. and G. Wendler 1988: Research results from Antarctic Automatic Weather Station. *Review of Geophysics*, **26** (1), 45-61
- Vowinkel,E. and S. Orvig 1962: Relation between solar radiation income and cloud type in the Arctic. *J of Applied Meteorology*, **1**, 552-559
- Wendler, G. and T. Quackenbush 1996: UV radiation in the southern seas in early Spring 1993. *Theoretical and Applied Climatology*. **53**, 221-230
- Wendler, G., B. Moore, B. Hartmann, M. Stuefer and R. Flint 2004: Effects of multiple reflection and albedo on the net radiation in the pack ice zones of Antarctica. *J. Geophys. Res.*, **109**, DO6113, doi:10.1029/2003JD003927.